UNIVERSITI MALAYSIA PERLIS
International Journal of Nanoelectronics and Materials
IJNeaM
ISSN 1985-5761 | E-ISSN 2232-1535

Wet Chemical Synthesis of Anode Reforming Layer in Solid Oxide Fuel Cell: A Comprehensive Review of Sol-Gel, Co-Precipitation and Combustion Synthesis

Saidatul Haneen Badruhisham [a], Anis Muneerah Shaiful Bahari [a] *, Saidatul Akmal Biyamin [a], Nor Anisa Arifin [a] *, and Ng Guat Peng [a]

[a]*Material Engineering & Testing Group, Tenaga Nasional Berhad Research Sdn. Bhd, 43000 Kajang, Selangor, Malaysia*
∗*Corresponding author. Tel.: +60-19-911-0292; e-mail: muneerah.shaifulbahari@tnb.com.my; Corresponding author. Tel.: +60-16-426-0462; e-mail: NorAnisa.Arifin@tnb.com.my*
∗*S. H. Badruhisham and A. M. S. Bahari contributed equally to this work*

Received 1 December 2023, Revised 4 March 2024, Accepted 12 March 2024

ABSTRACT

Anode reforming layer is one of the common strategies to reduce the impact of natural gases as fuel for solid oxide fuel cells (SOFC). This anode reforming layer helps to convert natural gas, for example, methane to hydrogen during the operation of SOFC. Thus, it reduces the formation of carbon deposition and increases the SOFC performance. However, the performance of the anode reforming layer depends on its microstructure characteristic, which may vary based on the synthesis method. Synthesis methods, such as powder, infiltration, coating, and combination routes, are studied to produce an optimum catalyst material. Powder routes, which consist of dry and wet methods, are gaining popularity due to their performance, simple and low-cost method. However, the wet chemical method is favoured for its cost-effectiveness, simplicity, and ability to produce high-quality powder. Thus, this review discussed the wet chemical methods, specifically the sol-gel, co-precipitation and combustion synthesis methods. In addition, the common parameters, previous findings and modifications of these methods were also briefly discussed. This review aims to discuss the various anode reforming layer synthesis methods, a general comparison of the methods and their influence on the properties and performance of SOFCs.

Keywords: *Anode reforming layer, Wet chemical synthesis, Solid oxide fuel cell*

1. INTRODUCTION

Energy is essential for human's everyday activities. Other elements contributing to an increase in energy demand are the rapid rise of the total population and steady personal income growth. In Malaysia, the primary contributors to energy consumption are distributed among several sectors, namely transportation, industrial, non-energy, residential, and agricultural. These sectors collectively account for the significant portion of the nation's future energy utilization. Increasing energy consumption and depleting fossil fuel availability are the key issues, together with concerns about the impact of using conventional fossil fuels on human health [1]. As a result, specific settings are required to adopt renewable energy sources, including solar, wind, hydroelectric, and geothermal. These sources need a supportive energy storage tool to keep excessive energy where in the current situation, batteries are essential for portable power operation. Nonetheless, over extended periods of use, batteries pose environmental hazards due to the presence of flammable substances and toxic electrodes. On the other hand, fuel cells offer a better energy conversion technology that can function in any environment, have almost zero emissions, noise-free and efficient [2]. Its attractive features such as durability, clean energy over the long term, fuel cell-based power generation systems have attracted significant interest from all fields of academia and industries [3].

Fuel cells are electrochemical devices that convert chemical energy directly into electrical energy [1], [2], [3], [4], [5]. Fuel utilization efficiency in fuel cells can reach up to 85% [2]. The primary benefits of this technology are energy conversion procedures that reduce environmental air pollution without employing the combustion process [6]. Renewable fuels, such as hydrogen, methanol, and ethanol readily available in nature and easy to manufacture through fermentation, qualify fuel cell technology as a sustainable and dependable energy source. Additionally, this technology lessens the dependent on fossil fuels like gasoline [7]. Another plus point of fuel cells is that they can operate in regenerative mode, changing excess electrical energy back into chemical energy [8]. This characteristic allows fuel cells to pair up with renewable energy sources like solar and wind to generate constant electricity [2]. Therefore, research into diverse fuel cell technologies is ongoing globally. The solid oxide fuel cell (SOFC), one of many fuel cell types, has drawn much attention because of its high efficiency and minimal environmental pollution emissions.

SOFCs are potential electrochemical energy conversion devices that operate at high temperatures, typically between 600 and 900 °C [4], [5], [9], [10]. High electrical conversion efficiency and fuel flexibility are just a few benefits of the high working temperature [9]. A nickel-yttria stabilized zirconia (Ni-YSZ) cermet is now the most commonly used anode in SOFCs due to its excellent electrochemical activity for hydrogen oxidation and proven long-term durability at SOFC operating conditions [2], [4], [5], [11], [12]. In order to continue to be successful economically, SOFCs will need to run on carbonaceous fuels and be resistant to common impurities in those fuels [13]. Carbon and sulphur are two of the most frequent poisons, and conventional anodes made of composites of Ni-YSZ are not resistant to both, leading to long-term deterioration [2], [5], [13]. For the next generation of SOFCs to effectively compete with traditional power plants at the grid scale with boilers and combustion engines at lower scales, carbon (from the fuels) and sulfur (contaminants) tolerance needs to be optimized from time to time. Table 1 shows the power density of reported hydrocarbon-fueled SOFC. In the future, SOFCs operating directly on hydrocarbon fuels without external reforming are anticipated to play a significant role in energy generation. However, employing hydrocarbon fuels has some problems for the Ni-YSZ anode, mainly the carbon deposition [2], [5], [12], [14].

Carbon deposition in an anode can cover the active areas of the anode, resulting in a rapid drop in cell performance [2], [5]. According to Kumar *et al.*, reducing the operating temperature, adjusting the steam and carbon ratio, and creating new anode catalysts are potential strategies for overcoming carbon deposition [2]. A high steam-to-carbon ratio is indeed to prevent carbon from depositing. However, it reduces the system's electrical effectiveness and various substitute materials were studied as prospective anodes in recent years to address Ni-YSZ cermet anode's drawbacks. [2], [12].

For many years, a substantial area of research on the application of catalytic reforming layer and internal catalyst in the processing of fuels, as indicated in Figure 1 [2]. Carbon and sulphur significantly impact the catalyst's effectiveness in fuel catalytic processes. Under specific circumstances, this effect can be very significant, where the catalyst deactivates quickly, resulting in unfeasible and/or expensive processes [13]. Due to these limitations, significant research has been devoted in developing an on-cell catalytic reforming layer (OCRL) and or known as an anode reforming layer, that is resistant to sulphur poisoning and carbon deposition [5], [12], [15]. The anode reforming layer is regarded as the most promising methane reforming design for hydrocarbon-fueled SOFC due to its simplified system, coking resistance, material variety and low cost [15]. The effectiveness of the catalyst depends on the synthesis method to provide a suitable material for the anode reforming layer. This literature may briefly compare the anode reforming layer synthesis method specifically for the wet chemical process.

The main objective of this review is to summarize on different wet chemical process synthesis methods of SOFC anode reforming layer. An introduction to the anode reforming layer, the hydrocarbon mechanism in SOFC, and other synthesis methods will also be discussed briefly.

Table 1. Power density of reported hydrocarbon fueled SOFC

No.	Fuel	Chemical composition	Common sources	Temperature (°C)	Highest power density (W cm^{-2}) reported based on synthetic simulated gas
1	Hydrogen	H_2	Fossil fuels (natural gas), renewable energy or biogas	650	1.960 [16]
2	Liquefied Petroleum Gas (LPG)	C_3H_8/C_4H_{10}	natural gas, oil extraction, co-product of oil refining or made from waste or renewable vegetable oils	800	0.973 [17]
3	Methane	CH_4	Pure industrial methane	800	0.550 [18]
4	Ammonia	NH_3	Soil from bacterial processes, decomposition of organic matter including plants, animals and animal wastes	800	0.380 [19]
5	Methanol	CH_3OH	Carbon-based feedstocks such as biomass, natural gas, and coal	750	0.360 [20]
6	Natural gas	CH_4 (75-98%)	Fossil fuels	750	0.317 [21]
7	Ethanol	C_2H_6O	Corn or cellulosic feedstocks (crop residues and wood)	700	0.280 [22]
8	Biogas	CH_4(50–75%) + CO_2	Waste or landfills	800	0.245 [23]
9	Diesel	$C_{\sim13}H_{\sim24}$	Crude oil or biomass	900	0.140 [24]
10	Gasoline	C_8H_{18}	Crude oil or other petroleum liquids	750	0.031 [25]

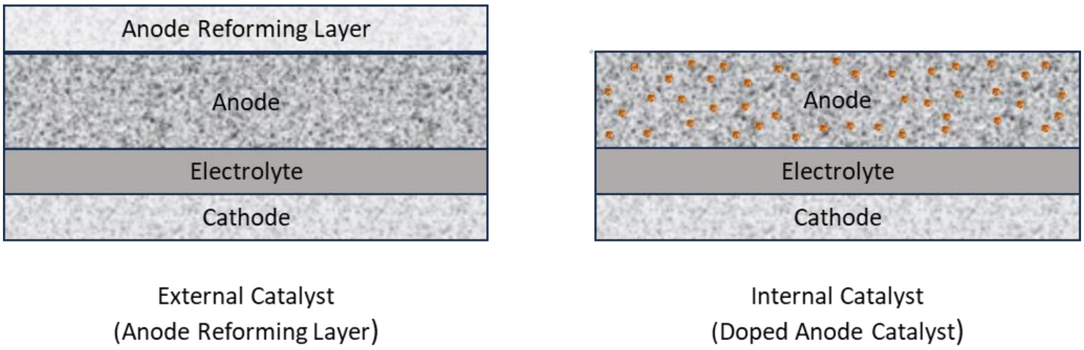

Figure 1. Anode catalyst method

2. ANODE REFORMING LAYER

Anode reforming layers is one of the most effective strategies for combating carbon deposition limitations. A porous additional layer is applied on the anode support so that the hydrocarbon fuel that first enters the layer undergoes a reforming reaction by the anode reforming layer. The hydrocarbon fuel is converted into syngas, which reduces carbon deposition significantly. The rest of this review will give a detailed explanation of the mechanism that occurred during the conversion of hydrocarbon fuel into syngas.

A few other successful strategies to overcome carbon deposition are by changing the operating parameters and adding nanocatalysts in the anode as well as the (Y, Ce)O_{2-d}(YDC) layer between the anode and electrolyte [2], [15]. Adding a YDC layer would interfere with the current optimum fabrication process on Ni-YSZ SOFC because it is a process that must be added between the anode and electrolyte. Besides that, changing the operating temperature of SOFC, such as lowering it and increasing current loading, would produce adverse effects, such as reducing cell power output and fuel utilization [15]. Thus, adding a nanocatalyst on the anode or an anode reforming layer would be some of the best options to overcome carbon deposition in SOFC.

2.1. Hydrocarbon Mechanism

In the hydrocarbon mechanism, hydrogen gas is currently the primary fuel source for fuel cells. However, since 96% of hydrogen gas is made from hydrocarbons, it would be simpler if fuel cells could directly utilize these sources [26], [27]. Natural gas and biogas containing methane and trace amounts of other hydrocarbons are particularly cost-effective and popular for most stationary SOFC systems [27], [28]. Their preferability is due to the inexpensive and easily accessible offers of a more affordable and practical way to produce power [28], [29], [30]. Biogas primarily contains 50-70% of methane (CH_4), 25-50% of carbon dioxide (CO_2), less than 10% of water (H_2O), and 2-8% small amounts of additional pollutants such as hydrogen sulfide (H_2S) and ammonia (NH_3) [29].

2.2. General Reaction of SOFC

The system's performance would be enhanced and kept simple by directly using hydrocarbons such as methane in a SOFC without requiring a preceding reforming step to make hydrogen. The general reactions for hydrogen-fueled SOFC are only the electrochemical conversion to electricity, heat and the reaction to produce water as a byproduct, as shown in Equation (1) [31].

$$H_2 + \frac{1}{2}O_2 \rightarrow H_2O \tag{1}$$

Equation (1) is the derivatives from the overall chemical reaction of hydrogen-fueled SOFC. The cathode reduces O_2 and has enough conductivity to supply the reaction with electrons [32], [33], [34]. O_2 subsequently oxidizes the fuel as it passes through the anode's Triple Phase Boundary (TPB) via the electrolyte [32]. The electrochemical reactions can also be written as:

Oxidation of hydrogen gas at the anode side:

$$H_2 + O^{2-} \rightarrow H_2O + 2e^- \tag{2}$$

Reduction of oxygen gas at the cathode side:

$$O_2 + 4e^- \rightarrow 2O^{2-} \tag{3}$$

2.3. Direct Utilisation of Hydrocarbon

On the other hand, a carbon-fueled SOFC involves complicated reactions due to the presence of a variety of species of gas, which are methane (CH_4), hydrogen (H_2), carbon dioxide (CO_2), carbon monoxide (CO) and carbon (C) [10]. The main differences between hydrogen and carbon-fueled SOFCs are the input from the anode side and their byproducts, which may involve carbon, as shown in Equations (4) and (5) [31].

Anode side reaction when using a hydrocarbon as fuel:

$$CO + O^{2-} \rightarrow CO_2 + 2e^- \tag{4}$$

$$CH_4 + 4O^{2-} \rightarrow 2H_2O + CO_2 \tag{5}$$

Equations (6) and (7) show the steam and the dry reforming reaction, respectively [10]. Based on these equations, both produce hydrogen and carbon monoxide [27], [32], [33], [35], [36]. Among these reforming reactions, steam methane is the most widely established technology for hydrogen production [33], [35], [37].

Steam methane reforming reaction:

$$CH_4 + H_2O \leftrightarrow 3H_2 + CO \tag{6}$$

Dry reforming reaction:

$$CH_4 + CO_2 \leftrightarrow 2H_2 + 2CO \tag{7}$$

The decomposition of methane at high temperatures [Equation (8)] produces solid carbon and hydrogen gas [29], [32], [33], [37]. It was reported in a previous study that methane decomposition [Equation (8)] can occur on the anode substrate (AS) and at the anode functional layer (AFL) [27], [31]. Besides that, Equation (9) (Boudouard reaction) also forms solid carbon when SOFC operates below 600 °C [29], [35]. The combination of high-temperature methane decomposition and carbon oxidation by carbon dioxide [Equation (10)] produces the dry reforming reaction [Equation (7)] [37]. The dry reforming reaction will likely happen when SOFC is fed with biogas containing CH_4 and CO_2 [32]. Furthermore, water produced by Equation (1) or supplied can react electrochemically with carbon, as shown in Equation (10), producing carbon monoxide [26], [37]. Unbalance of Equation (8) and Equation (10), in the case of less carbon undergoing oxidation, might lead to excess carbon remaining on the catalyst surface, which would form a carbon deposit that would deactivate the catalyst on the anode [31], [37]. Carbon buildup has the potential to obstruct pores and expand the anode, harming the SOFC [26], [29].

Methane cracking reaction:

$$CH_4 \rightarrow C + 2H_2 \tag{8}$$

Boudouard reaction:

$$2CO \leftrightarrow C + CO \tag{9}$$

Carbon deposits can be eliminated by carbon oxidation using CO_2 [Equation (10)] or steam [Equation (11)], as long as the oxygen sources are available. Additionally, the water-gas shift (WGS) reaction [Equation (12)] (or the reverse process) may also occur at high operating temperatures in addition to the reforming reaction, which could further convert CO to CO_2 [10], [31], [32], [35], [36].

Carbon oxidation by CO_2:

$$C + CO_2 \leftrightarrow 2CO \tag{10}$$

Carbon oxidation by H_2O:

$$C + H_2O \leftrightarrow CO + H_2 \tag{11}$$

Water-gas shift reaction:

$$CO + H_2O \leftrightarrow CO_2 + H_2 \tag{12}$$

After introducing the anode reforming layer at the operating temperature is higher than 600 °C, the hybrid reaction of steam methane and dry methane reforming could occur internally, which might be maximizing the production of H_2 [10]. Simultaneously, the high methane conversion rate can reduce the methane concentration entering the anode, thus, preventing coking [15]. The electrochemical reaction [Equation (1) and Equation (4)] occurs more frequently in the AFL region, where there are more TPB areas [31]. The reactions that occurred in hydrocarbon-fueled SOFC are summarized in Figure 2 [33] and synthesis method for anode reforming layer will be elaborated in the next section.

3. ANODE REFORMING LAYER SYNTHESIS METHOD

Since the anode reforming layer acts as a catalyst for the SOFC, a few requirements must be met, including match thermal stability, chemical compatibility, specific area, and particle size [2]. Various methods have been used to synthesis SOFC anode reforming layer to gain desired properties (fine particle size, specific surface area, right material composition, etc.), as shown in Figure 3. For instance, powder, infiltration, coating and combination route can be divided into sub-methods. Each method has

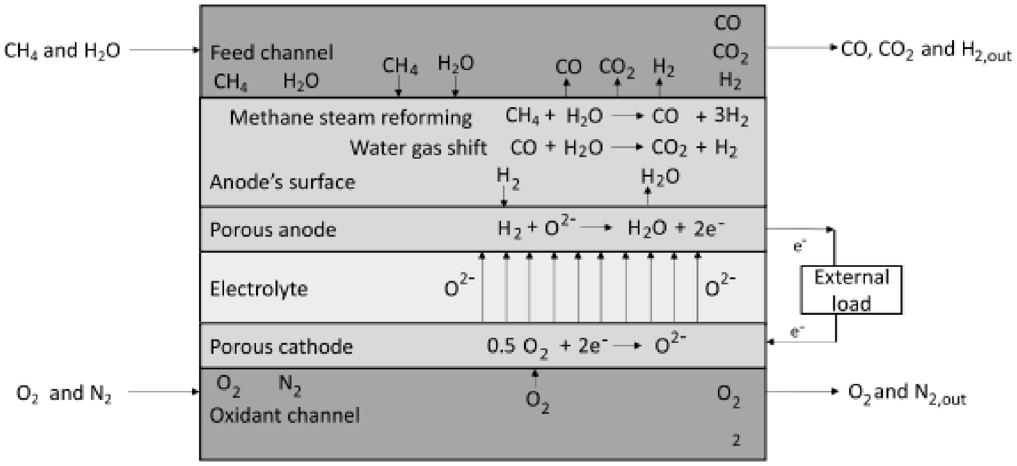

Figure 2. Electrochemical reactions on hydrocarbon-fuelled SOFC (Reprinted with the permission from Ref. [33], Copyright (2022), Elsevier)

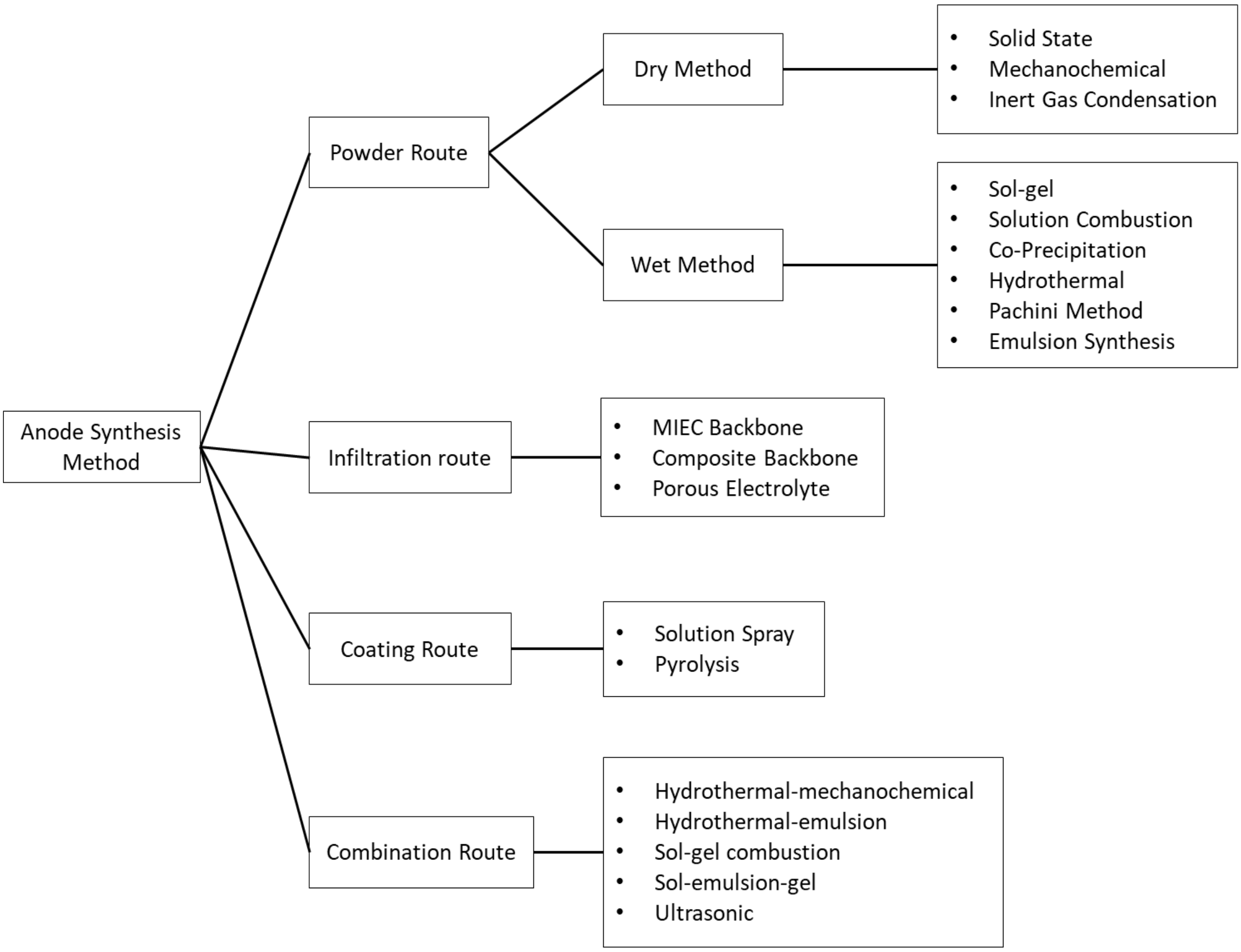

Figure 3. Anode reforming layer synthesis method

specific attributes to nanoparticle characteristics, manufacturing speed, cost, feasibility, and environmental impact [38]. Thus, the selection of the synthesis method is crucial as the anode reforming layer microstructure, porosity, morphology, particle size distribution, shape, and TPB are all affected by the synthesis process.

Other than that, this synthesis method also can be classified into top-down and bottom-up [39]. The top-down approach converts bulk material into small-sized particles, while the bottom-up is the formation of nanoparticles from smaller molecules [39]. The characteristics of the synthesized anode reforming layer material can be improved by understanding the benefits and drawbacks of each method. Some techniques are quick, inexpensive, easy to use and environmentally friendly. Therefore, understanding these techniques can improve the anode reforming layer component's performance and, by extension, the performance of the entire SOFC system. Table 2 shows the comparison of the anode reforming layer synthesis method.

Based on Wang et al. [38], solid-state reactions are suitable for mass production due to their simple process, eco-friendly and economical method. This method can be affected by the reaction time, reaction pressure, reaction atmosphere, and cooling speed. Senthil et al. [2] found that solid-state reactions have a major drawback which is challenging to control the particle size that will extend the TPB length and increase the electrochemical activities.

Ball milling or mechanochemical synthesis is a solid-state synthesis method used to decrease the size of the particle. Although the synthesis has limitations, the procedure is easy and uses cheap raw material, making it suitable for large production powder [39]. Apart from that, mechanochemical is also quite similar to the solid-state ratio. But mechanochemical is much simple and able to produce a well-defined powder. For this method, parameters like time, material type, milling ball size, and momentum can affect the quality of the powder [38].

Rafique et al. [39] concluded from the previous research that hydrothermal synthesis able to control particle grain size, morphology, crystalline phase, surface chemistry, and reaction temperature. Four critical factors affecting particle size and morphologies in hydrothermal synthesis are hydrothermal temperature, time, organic additive, and solvent [38]. Hydrothermal and Solvothermal are similar methods with different reactants: water and organic solvent [40]. The pyrolysis method or spray pyrolysis is one of the famous methods in the coating route. This method will produce non-agglomerated, refined, and homogeneous powder [41]. In the case of pyrolysis, material composition, process temperature resident time will affect the process [38]. The general illustration of the synthesis route for catalyst is shown in Figure 4.

Based on the review from previous research, the dry and wet methods are the most potential methods to synthesise

Table 2. Comparison of the synthesis method [38], [39], [41], [42], [43], [44], [45]

Route	Method	Advantage	Disadvantage	Affected Parameter
Powder Route (Dry Method)	Solid State	- Simple method - Eco friendly - Pure and stable product - Inexpensive	- Produce particle with irregular shape - High agglomeration - Inhomogeneous shape, size - Require high temperature - Time consuming	- Reaction time - Reaction pressure - Reaction atmosphere - Cooling speed
	Mechanochemical	- Increase TPB length - Produce well defined structure - Simple and efficient method	- Sensitive particle - Possible of contamination - Time-consuming - Non-uniform distribution of metal	- Time - Material type - Milling ball size - Momentum
	Ball milling	- Large scale production - Simple and economical - Cost-effective - Suitable for both wet and dry materials - Produce fine powder	- Require high energy - Time consuming - Possible of contamination - Inhomogeneous shape, size	
	Inert gas Condensation	- Excellent quality control	- Low production rate	
Powder Route (Wet Method)	Sol-gel	- Control the processing parameter (size, morphology) - Eliminate impurities & agglomeration - Low-cost equipment - High purity - Ultra-fine particle - Simplest method	- Long drying process - Expensive starting material for large scale	- Ph value - Stirring speed - Reaction temperature
	Combustion	- High purity - Flexible usage of fuel - Low-cost instrument - Homogenous powder - Ultrafine powder - High energy efficiency	- Difficult to scale-up and estimate the size and amount of particles - Form aggregation	- Ignition temperature - Synthesis time - Reactant mixture - Fuel
	Co-precipitation	- Can control particle size & composition - Cost effective among wet method - High purity - Better homogeneity - Less agglomeration - Fine-grain size	- Not suitable to certain material - Less effective for low solubility reactant - Time consuming - Insufficient control of size and shape distributions	- Temperature - Ph value - Type of solvent - Mixing rate - Post treatment - Precipitation agent
	Hydrothermal	- Low temperature - High purity and crystallisation - Better particle size and morphology - Better homogeneity - Less agglomeration	- Uncontrollable aggregation - Slow reaction rate - Complicated experimental procedure	- Temperature - Time - Organic additive - Solvent effect
	Pachini Method	- High-purity powder - Homogenous - Simple method		
Infiltration Route	MIEC Backbone			
	Composite Backbone	- Stabilise the morphology of the nanoparticles		
	Porous Electrolyte	- Improve cell performance		
Coating Route	Solution Spray	- Consistent particle size - High purity		
	Pyrolysis	- Cost-effective - Industrially scalable - Simple method - Pure coting - High surface area	- Wide size distribution - Aggregation - High energy consumption - Poor mechanical stability	- Material composition - Temperature
	Electroless coating	- Can deposited most of the composite which thermodynamically favourable	- Limited research on this method	
	RF Sputtering	- Increase TPB - Economical - Less impurities	- Poor surface morphology	

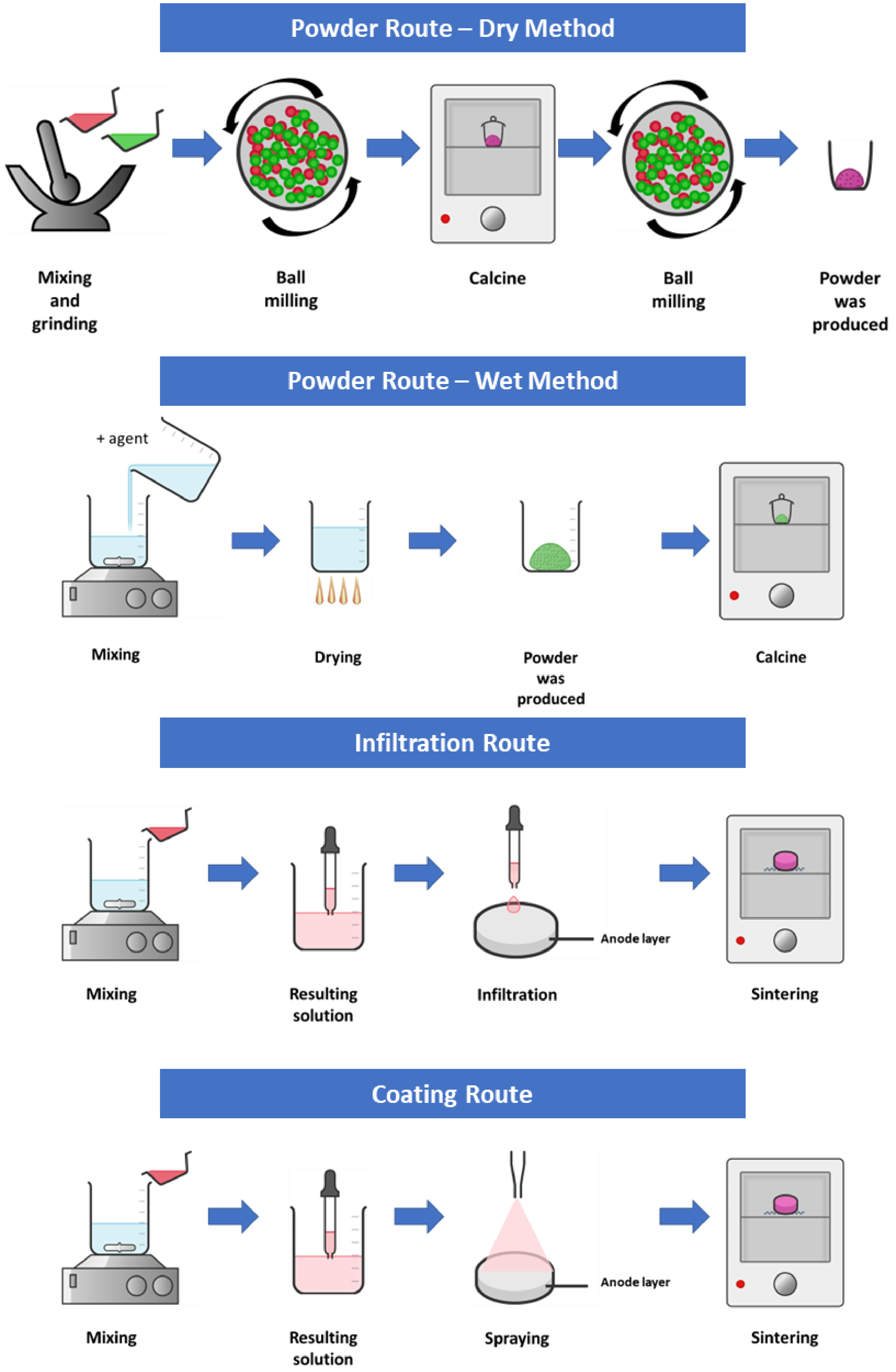

Figure 4. General illustration of the synthesis route for catalyst

anode reforming layers as they are the easiest. It is also vastly used in synthesis due to its simple procedure and eco-friendly. On the other hand, the dry method outcome is prone to particle shape irregularity, contamination, laborious, and cost-extensive. The wet chemical method has a significant advantage over other methods due to the inexpensive powder process cost involved in atomic-level mixing and homogenous powder [2]. Therefore, based on the review, the most suitable approach to synthesis an anode reforming layer is the wet chemical method (sol-gel, co-precipitation, combustion) as it is simple, cost-effective, produces high purity and consistent particles. The details of these methods will be discussed in the next section.

4. WET CHEMICAL METHOD

The three most commonly used wet chemical methods; sol-gel, co-precipitation and combustion, will be discussed in detail. Figure 5 shows a simple comparison of the general methodology of these three methods.

4.1. Sol Gel

Another popular synthesis method for catalysts is the sol-gel method. It has been widely used to synthesis organic, biomaterial, and ceramic material and has been gaining attention in SOFC applications [15], [40]. Sol-gel is a process from liquid to solid involving hydrolysis and condensation, usually forming a gel.

Table 3 shows the previously reported studies on anode reforming layers synthesized using the sol-gel method. Sol-gel consists of two primary materials: the precursor (or salt) and the chelating (reducing or complexing) agent. The common practice of the sol-gel method is to prepare a precursor solution [46], [47], [48], [49], [50]. The chelating agent is then added to a fully dissolved precursor solution. Then, gelation occurred due to the chelating agent's reaction, increasing the solution's temperature, which produced hydrogel. The hydrogel undergoes drying to obtain either xerogels or aerogels in powder form. For SOFC fabrication, the resulting powder undergoes further calcination to produce an anode-reforming layer, as shown in Table 3 [46], [47].

As shown in Table 3, the commonly used precursors are nitrates, which are well-known to produce high-conductivity nanopowder [40]. However, a few studies also explored the effect of using different types of precursors, such as oxide, lactate, acetate, citrate and gluconate, in enhancing the process of sol formation [51], [52], [53]. Besides that, as shown in Table 3, citric acid, acetic acid, EDTA and TEOS, are the common chelating agents used, with the help of ammonia solution or nitric acid, to adjust the pH of the solution. Most previous studies used distilled water as a solvent except for Bej *et al.,* which uses ethanol to dissolve TEOS [54]. Thus, it can be suggested that the common parameters for sol-gel methods are the chelating agent, stirring method, pH of the solution before gelation, heat treatment (ageing and drying), and calcination temperature, as shown in Table 3.

The main advantages of sol-gel are its ability to produce high-purity and ultrafine powders that can reduce air

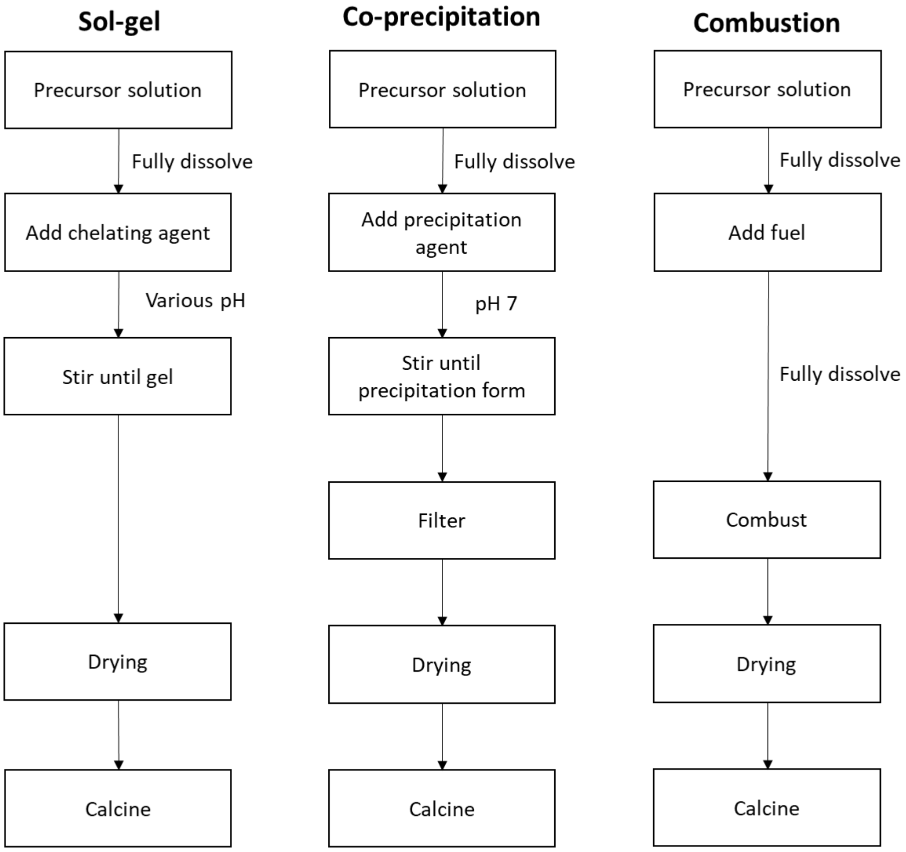

Figure 5. General methodology of sol-gel, co-precipitation and combustion method

pollution (do not emit carbon dioxide) and prevent impurities and agglomeration [40]. However, the sol-gel method has a few drawbacks, including a long drying process and an expensive starting material that does not suit large-scale production. Other than that, volume shrinkage and cracking issues were also reported due to the complex reaction of gelation and drying. Parameters such as the optimum chelating agent, drying rate, and thickness are being studied to avoid shrinkage and cracking issues [40]. Furthermore, some chelating agents lead to instant gelation in the presence of water, thus, extra control and strict supervision are necessary for the sol-gel method.

Nevertheless, as shown in Table 3, modification of the sol-gel method had been explored, as seen in the citric acid-nitrate, the EDTA-citrate and Pechini methods had been introduced to overcome the drawbacks of the conventional sol-gel method. In 2012, Wang et al. studied sucrose and pectin as substitutes for conventional, expensive chelating agents [55]. Both sucrose and pectin are environmentally friendly, easy to store, inexpensive and available in the market. The environmentally friendly sol-gel method could synthesis highly porous and stable composite anodes. Furthermore, the EDTA-citrate sol-gel method, which uses citric acid and EDTA as chelating agents, shows positive mixing as it may help to enhance the reaction rate of the material at the molecular level [40], [56]. At the same time, the Pechini method is famous for producing homogenous pure nanopowders at a lower temperature. The synthesized material demonstrated medium carbon deposition, good conductivity and good catalytic activity [40].

Another new modified sol-gel method is the sol-gel-in situ exsolution. The catalyst (after calcination and reduction) is uniformly dispersed by active, stable nanosized components on the surface [15]. The embedded dispersed component was suggested to increase the interaction, which can enhance the catalyst coking resistance and improve the performance of methane steam reforming (MSR) [56]. The sol-gel method can potentially synthesis an excellent anode-reforming layer based on the positive results obtained.

4.2. Co-Precipitation

Co-precipitation is one of the wet methods in anode synthesis due to its cost-effectiveness compared to other methods. This method offers less agglomeration, increased surface area, and high purity. Co-precipitation can be categorized into two types of precipitation; hydroxide (limestone, sodium carbonate, sodium hydroxide, sodium decanoate) and sulfide precipitation method. Hydroxide precipitation agents release hydroxide ions, changing the metal to form insoluble hydroxide precipitation [57].

Metal substances first dissolve with the distilled water, thoroughly mixed, and stirred at specific temperatures. Precipitation agents such as sodium hydroxide, ammonia, and oxalic acid were used to form the precipitation synthesis. Precipitation agent selection is one of the crucial things for successive rates of calcination and sample shaping [58]. The precipitation is washed with water or ethanol to remove free water and other impurities [59]. The sample was dried in the oven before being calcined in the furnace at high temperatures which usually 500 °C and above. The powder structure, such as crystallization, size, surface area, and morphology, can be measured via X-ray diffraction (XRD) analysis, Transmission Electron Microscopy (TEM), Brunauer-Emmet-Teller (BET) surface area analysis and others. Table 4 shows the comparison study of the co-precipitation method.

According to Ju Hee *et al.* [59], co-precipitation only requires low calcination temperature and highly homogenous and uniform particles compared to other methods. The test of the sample of CeScSz by TGA analyses the activation point for the crystallization the powders. The activation point indicates the minimum calcination temperature of this powder was 400 °C. Additionally, as the calcination temperature increases, the crystalline size increases, decreasing specific surface area, grain size growth, and agglomeration increase under the same lattice constant. Zhu *et al.* [57] also mentioned that the co-precipitation method might produce secondary pollution due to an additional large amount of precipitation agent during the process.

Fariza *et al.* [60] conducted an XRD analysis to investigate the crystallographic structure, chemical composition, and properties of samarium doped ceria. The author concluded that the crystallization growth of the co-precipitation synthesis process grew faster, but the size distribution range varied widely than other synthesis methods. Furthermore, the band intensities of the peak also decrease as the calcination temperature increases. Peak band intensities show the residual bond in which the purity of the powder increases if the temperature increases [60]. In conclusion, calcination temperature significantly impacts the synthesis, and it is to be noted that every material has its range of calcination temperature.

In addition, Spiridigliozzi *et al.* [58] found that the solution's molar ratio and mixing rate affect the Sm-doped ceria co-precipitation method. Slow mixing and variable molar ratio can cause different formations of crystalline phases. Fast mixing causes amorphous regardless of molar ratio value. Besides this, considering the calcination temperature, ceria-based co-precipitation tends to form a crystallized structure at room temperature. The author also studies the impact of sintering for sampler powder of Sm-doped and Gd-doped ceria by co-precipitation. Specifically, the powders made from the crystalline co-precipitates have unsatisfactory densification and exhibit deplorable sintering behaviour due to agglomeration in the powder during the synthesis process. Therefore, the powder will be porous, prolonging the thermal treatment [58]. The precipitation agent significantly affects the co-precipitation method as it will determine the success of this method. According to Table 4, ammonium hydroxide is the common precipitation agent opted in many methods because of the quality of the powder produced. The co-precipitation process can be stirred at room or specific temperatures depending on the reactant. The major drawback of this method is sometimes it does not apply to various materials, and it is difficult to repeat the process.

Co-precipitation can produce monodispersed nanoparticles and high-performance anodic material in a short time [41]. Nevertheless, particle size, shape, and sintering density depend on the reaction temperature [41]. In this method, the parameters that will affect the quality of the powders are temperature, pH value, solvent type, mixing rate of solvent, and post-treatment. Based on the parameters affected, it is challenging to control the size particle in this method [38]. Other than that, co-precipitation also requires a long time, sometimes incompatible with many materials. This method is also ineffective when it involves different reactant solubilities. Hanisah et al. [45] found that inadequate control of size and shape distribution is the major drawback of this method. Besides, the type of precipitation agents plays a crucial role in the powder's dispersibility, shape, and size of the particles. The study found that ammonium bicarbonate was the best precipitation agent that produced homogenous powder with the smallest particle size and lowest degree of agglomeration to increase the anode electrochemical performance. [45]

4.3. Combustion

The combustion method is one of the most common methods for wet chemical processing. The combustion method is preferable due to its homogenous microstructure, as the oxides were prepared together [40]. The advantages of using the combustion method are that it is inexpensive, less time-consuming (as it usually does not consist of an ageing or drying process), simple and can produce a high-yield ultrafine nanopowder [39], [40], [60], [61]. Combustion methods such as the conventional glycine-nitrate process (GNP) and solution combustion synthesis (SCS) are the two most common methods to synthesis an anode reforming layer. The combustion method can be categorized as a process method based on the type of fuel used.

The basic mechanism of the combustion method is that the metal solution, or the oxidizer, is combusted using fuel to form metal oxide. Distilled water is used to dissolve the oxidizer. Table 5 shows that metal nitrate oxidizers are commonly used due to their high solubility in water, which can lead to a homogenous solution [40]. The homogenous aqueous solution of oxidizers was first mixed by stirring until fully dissolved. Fuel was then added, followed by constant stirring. The stirring or mixing time depends on the solubility and method, which can vary due to the different materials used, as shown in Table 5. Some studies include heating during mixing to obtain a viscous gel before combustion [62], [63], [64], [65]. Then the resulting solution or gel undergoes combustion at 200 °C to 300 °C, except for Shetty *et al.,* which conducted combustion at 500 °C.

Based on Ghahramani *et al.,* the fuel type plays a vital role in combustion as it can influence the reaction rate. Compared to other fuels, glycine has a higher heat of combustion, which is why it is common [62]. On the other hand, the samples that used a low-combustion heat fuel, such as urea, led to an incomplete reaction, forming unwanted compounds. The XRD patterns, microstructure characterization and particle size also depend on the type of fuel used, such as low combustion heat, which may produce a smaller crystallite size and low grain growth [62].

GNP is a process that uses glycine as fuel and nitrate as an oxidizer. It is an attractive method due to its simple preparation, inexpensiveness (glycine is one of the cheap amino acids), rapid heating rate, and short reaction time [40]. Fast reaction time was reported in producing large quantities of different parts used in SOFC fabrication [40]. Even though a short time is needed to obtain the reaction, the mixing time of the solution of glycine and nitrate needs to be noted as it is essential to obtain a pure phase material [66]. A longer mixing time can increase the potential for homogenous combustion.

Another highlight of GNP is that the sample produced may not need to undergo calcination as combustion has already formed an oxide [61], [62], [67]. Based on Ghahramani *et al.,* the sample produced by glycine resulted in well-crystallized nanoparticles due to its high exhaust gas volume and combustion reaction [62]. The resulting sample was observed to have a highly non-uniform agglomeration and porous, spongy-like morphology, which is inevitable for the combustion method [60], [62].

A study by Wang *et al.* (2014) exploring the different synthesis methods to synthesis NiFeCu alloy anode catalysts suggested that the catalyst synthesized using GNP displayed the highest catalytic activity for the partial oxidation of methane. Still, for the long-term actual testing, catalysts synthesized using the impregnation method showed excellent operational stability on methane fuel without decay for 100 hours [64]. However, the performance of the catalyst does not solely depend on the synthesis method, as a lot of studies have also suggested that a catalyst prepared using GNP exhibited better operational stability, higher coke resistance and a lower degree of graphitization (carbon deposit) compared to a catalyst prepared using the impregnation method [65], [68].

Kalyk *et al.* suggested that GNP may create an agglomerate of porous nanocrystalline particles due to its radical ignition, which may produce non-homogenous particles [60]. However, the mentioned microstructure did not hinder the performance of GNP, as it can produce the highest quality $Ce_{0.8}Sm_{0.2}O_{2-\delta}$ electrolyte based on its electrical properties compared to co-precipitation and the sol-gel method [60]. Thus, it can be suggested that combustion methods are suitable to synthesis compounds for SOFC fabrication, except that they may produce a non-uniform agglomerate nanopowder. However, much research has been done to modify GNP (particle-dispersed GNP) to enhance its densification, producing strong bonding and leading to less agglomeration [40]. In combustion, parameters such as ignition temperature, synthesis time, and reactant mixture can affect all particle properties [38]. Nevertheless, glycine is the best fuel due to the higher heat of combustion and cheapest fuel [44].

Table 3. Previous reported studies on anode reforming synthesised using sol-gel method

Year	Author	Method (name used in literature)	Precursor involved	Type of metal salt used	Solvent	Chelating/ reducing/ complexing agent	Stirred	Aged	Dried	Calcined	Ref.
2020	Koettgen *et al.*	Sol-gel	Sm, Gd, Ce	Nitrate	DI water	Citric acid	Stirred at 50°C for several hours until gelation. Then, temperature was increased to 120-150°C until foaming.	-	350°C for 3h	1000°C for 4h	[46]
2020	Qiu *et al.*	Sol-gel	Sr, Fe, Co, Mo	Nitrate	DI water	EDTA, citric acid, ammonia solution (pH ~8)	Stirred and heated until gelation.	-	-	1050°C for 5h	[69]
2019	Itkulova *et al.*	Pechini sol-gel	Co, Pt, Zr, La, Al	Nitrate	DI water	Citric acid monohydrate	Stirred at room temperature until fully dissolve. Then, the temperature was increased to 70°C until gelation.	-	110°C	400°C for 20h	[47]
2017	Zhao *et al.*	EDTA-citrate method	Mn, Co	Nitrate	DI water	EDTA, citric acid, ammonia solution (for pH)	Stirred at 80°C until gelation.	-	Pre-heated at 240°C for several hours	800°C for 6h	[70]
2016	Ma *et al.*	Sol-gel	Sr, La, Si	Nitrate, oxide	DI water	Dilute ammonia and nitric acid to adjust pH. TEOS, ethylene glycol, citric acid	Sr salt and TEOS was stirred for 1h. Followed with the mixing of all other chemicals which was stirred at 60-80°C for 3-4h.	-	120-150°C for 1.5h	800-1000°C	[51]
2014	Xu *et al.*	Sol-gel	Ni, Ca, Al	Nitrate, lactate	DI water	Acetic acid (pH 3)	Al salt and DI water was stirred at 85°C for 1.5h (500 rpm). The acetic acid was added, the temperature was increased to 95°C for 10h. Lastly, all of the other chemicals were added, the solution was stirred for 6 more hours.	-	110°C for 24h	850°C for 2h	[52]
2013	Bej *et al.*	Sol-gel	Ni, Si	Nitrate	Ethanol	TEOS	Stirred at room temperature for 5-6 h	Aged at room temperature for 1 week	110°C for 24h	350-500°C	[54]
2013	Xu *et al.*	Sol-gel	Al, Ca	Lactate, acetate, citrate, gluconate	DI water	Acetic acid (pH 3-4)	Stirred at 85°C for 1.5h (500 rpm). After acetic acid was added, the solution was stirred at 90°C for 24 hours.	-	110°C for 12h	900°C for 2h	[53]
2012	Wang *et al.*	Sol-gel	Ce, Gd	Nitrate	DI water	Sucrose, Pectin	Stirred for 1h. Then, the temperature was increase to ~90°C for 3h.	90°C for 24h	-	500-900°C for 2h	[55]
2010	Jin *et al.*	Citric acid-nitrate method	Cu, Mn	Nitrate	DI water	Citric acid	70°C for 24 h	-	400°C for 24h	950°C for 8h	[71]

*DI water: Deionised water, TEOS: Tetraethyl ortho-silicate, EDTA: Ethylenediaminetetraacetic

Table 4. Previous reported studies on anode reforming synthesized using Co-Precipitation method

Year	Author	Metal nitrate (oxidiser)	Salt / reducing agent/ precipitating agent	Stirred	Aging	Filter	Drying	calcine at	Ref.
2022	Futamura *et al.*	Ni, Co	Ammonia	at room temperature	-	filtered	100 °C for 10 hr in air	1000 °C for 2 hrs	[9]
2021	Nesaraj *et al.*	Gd,Sm, Ce, Co/Mn	Sodium hydroxide + DI water	at room temperature for 2 hrs		water/ethanol	60 °C overnight	300 - 1100 °C for 2 hrs	[72]
2020	Majewski *et al.*	Ni, Mo	Urea	95 °C for 4 hr	-	Water	room temperature	800 °C for 5 hrs and 1 hr heat treatment at 750 °C	[73]
2020	Dey *et al.*	Ce, Gd	Ammonium hydroxide	at room temperature	-	filtered		750 °C	[74]
2019	Gilbile *et al.*	Sm, Ce, O	Oxalic acid	at room temperature	at room temperature for 12 hrs	DI water	overnight	500 °C for 5 hrs	[75]
2018	Li *et al.*	Ce,Sm,Bi,O	Oxalic acid (pH 7)	at room temperature	-	distilled water + ethanol	at 80 °C	700 °C for 4 hrs	[76]
2018	Spiridigliozzo *et al.*	Ce, Gd, Pr	Ammonium carbonate		-		overnight	600 °C for 2 hrs	[58]
2014	Fan *et al.*	Gd, Ce, O	Ammonia, Hydrogen peroxide (pH 8-9)	80-90 °C	-	DI water + Ethanol	room temperature	600 °C	[33]
2012	Kang *et al.*	SZ, Ce, Sc	Ammonium hydroxide solution (pH 11-12)	at room temperature	room temperature for 24h	DI water + Ethanol	freeze-drying method at -20 to -85 °C	100 - 900 °C for 2 hrs	[59]
2010	Daza *et al.*	Ni, Mg, Al, Ce	Sodium carbonate (Ph 10.5)	60 °C (vigorous)	60 °C for 1 hr with stirring & 60 °C for 18 hrs without stirring	DI water	80 °C for 24 hrs	500 °C for 16 hrs	[77]

*DI water: Deionised water

Table 5. Previous reported studies on anode reforming synthesized using combustion method

Year	Author	Method (name used in literature)	Metal nitrate (oxidiser)	Salt type	Fuel/ reducing agent	Solvent	Stirred	Combusted at	Combustion occurred in	Dried	Calcined	Ref.
2020	Ghahramani *et al.*	SCS	Ce	Nitrate	Urea, glycine, glucose, citric acid	DI water	150°C until viscous gel obtained	300°C	Heater stirrer	-	-	[62]
2020	Kalyk *et al.*	GNP	Sm, Ce	Nitrate	Glycine	DI water	Stirred constantly	Not mentioned	Magnetic stirrer	-	200-1200°C (various temperature) for 5h	[60]
2019	Cheng *el al.*	GNP	Cu	Nitrate	Glycine	DI water	105°C @ overnight	200°C	Oven	-	-	[67]
2018	Somalu *et al.*	GNP	Li, Co, Zn	Nitrate	glycine	DI water	Stirred at room temperature for 40 min before adding fuel. Then, continue stirring for another 12h.	250-300°C	Hot plate	120°C for 12h	600°C	[66]
2018	Shetty *et al.*	SCS	Mg, Fe	Nitrate	Oxalyl dihydrazide (ODH)	DI water	Not mentioned	500°C	Muffle furnace	-	-	[61]
2014	Wang *et al.*	GNP	Ni, Fe, Zr, Cu	Nitrate	Glycine	DI water	Stirred until gel	240°C	Electric oven	-	850°C for 5h	[64]
2012	Zhu *et al.*	GNP	Ni, Fe	Nitrate	Glycine	DI water	Stirred until gel	240°C	Electric oven	-	850°C for 5h	[65]
2011	Wang *et al.*	GNP	Ru, Al	Nitrate	Glycine	DI water	Stirred until gel	240°C	Electric oven	-	850°C for 5h	[63]
2011	Wang *et al.*	GNP	Ni, Al	Nitrate	Glycine	DI water	Stirred until gel	240°C	Electric oven	-	850°C for 5h	[68]
2010	Wang *et al.*	GNP	Ni, Al, Ru, Ce	Nitrate	Glycine	DI water	Stirred until gel	240°C	Electric oven	-	850°C for 5h	[78]

*GNP: Glycine-Nitrate Process

5. CONCLUSION

The anode reforming layer is efficient to tackle the drawback of carbon deposition at the anode when using hydrocarbons as fuel. For this reason, the synthesis method plays a crucial role in providing a good material for anode reforming layer, as the efficiency of the SOFC depends on it. This study reviewed various synthesis methods, such as powder, coating, infiltration and combination routes, for preparing nanostructural components for SOFC. Some synthesis methods show excellent final products under various parameters for SOFC. However, there is a limited literature review on the synthesis method of the anode reforming layer, as it was recently introduced. Based on previous research, powder routes, which are dry methods and wet chemical methods, are the most popular methods for synthesizing an anode reforming layer as they show an improvement in performance and catalytic activity. However, the wet chemical method is commonly considered due to its low cost, simplicity and ability to produce high-quality powder compared to the dry method. Future work on comparing the effect of the wet chemical synthesis method on the performance of the anode reforming layer is recommended to produce the best catalyst for SOFC.

ACKNOWLEDGMENTS

The authors would like to acknowledge the support of TNB Research Sdn. Bhd.

REFERENCES

[1] N. Sazali, W. N. W. Salleh, A. S. Jamaludin, and M. N. M. Razali, "New perspectives on fuel cell technology," *Membranes (Basel).*, vol. 10, no. 5, 2020.

[2] S. Senthil Kumar and S. T. Aruna, "Hydrocarbon Compatible SOFC Anode Catalysts and Their Syntheses: A Review," *Sustain. Chem.*, vol. 2, no. 4, pp. 707–763, 2021, doi: 10.3390/suschem2040039.

[3] S. Kumaran, Z. Awang Mat, Z. Zakaria, S. H. Abu Hassan, and Y. Boon Kar, "A Review on Solid Oxide Fuel Cell Stack Designs for Intermediate Temperatures," *J. Kejuruter.*, vol. 32, no. 1, pp. 149–158, Feb. 2020, doi: 10.17576/jkukm-2020-32(1)-18.

[4] E. D. Wachsman and K. T. Lee, "Lowering the temperature of solid oxide fuel cells," *Science (80-.).*, vol. 334, no. 6058, pp. 935–939, 2011, doi: 10.1126/science.1204090.

[5] M. Andersson, H. Paradis, J. Yuan, and B. Sundén, "Review of catalyst materials and catalytic steam reforming reactions in SOFC anodes," *Int. J. Energy Res.*, vol. 35, no. 15, pp. 1340–1350, 2011, doi: 10.1002/er.1875.

[6] Z. Zakaria, Z. Awang Mat, S. H. Abu Hassan, and Y. Boon Kar, "A review of solid oxide fuel cell component fabrication methods toward lowering temperature," *Int. J. Energy Res.*, vol. 44, no. 2, pp. 594–611, 2020, doi: 10.1002/er.4907.

[7] Z. Zakaria, S. Kartom, K. Anuar, and A. Wahid, "The progress of fuel cell for malaysian residential consumption : Energy status and prospects to introduction as a renewable power generation system," *Renew. Sustain. Energy Rev.*, vol. 144, no. June 2020, p. 110984, 2021, doi: 10.1016/j.rser.2021.110984.

[8] J. Wei and J. Malzbender, "Steady state creep of Ni-8YSZ substrates for application in solid oxide fuel and electrolysis cells," *J. Power Sources*, vol. 360, pp. 1–10, 2017, doi: 10.1016/j.jpowsour.2017.05.113.

[9] S. Futamura *et al.*, "SOFC anodes impregnated with noble metal catalyst nanoparticles for high fuel utilization," *Int. J. Hydrogen Energy*, vol. 44, no. 16, pp. 8502–8518, 2019, doi: 10.1016/j.ijhydene.2019.01.223.

[10] L. Fan, C. Li, P. V. Aravind, W. Cai, M. Han, and N. Brandon, "Methane reforming in solid oxide fuel cells: Challenges and strategies," *J. Power Sources*, vol. 538, no. March, p. 231573, 2022, doi: 10.1016/j.jpowsour.2022.231573.

[11] J. Liu and S. A. Barnett, "Operation of anode-supported solid oxide fuel cells on methane and natural gas," *Solid State Ionics*, vol. 158, no. 1–2, pp. 11–16, 2003, doi: 10.1016/S0167-2738(02)00769-5.

[12] X. F. Ye, S. R. Wang, Z. R. Wang, L. Xiong, X. F. Sun, and T. L. Wen, "Use of a catalyst layer for anode-supported SOFCs running on ethanol fuel," *J. Power Sources*, vol. 177, no. 2, pp. 419–425, 2008, doi: 10.1016/j.jpowsour.2007.11.054.

[13] P. Boldrin, E. Ruiz-Trejo, J. Mermelstein, J. M. Bermúdez Menéndez, T. Ramírez Reina, and N. P. Brandon, "Strategies for Carbon and Sulfur Tolerant Solid Oxide Fuel Cell Materials, Incorporating Lessons from Heterogeneous Catalysis," *Chem. Rev.*, vol. 116, no. 22, pp. 13633–13684, Nov. 2016, doi: 10.1021/acs.chemrev.6b00284.

[14] G. Pongratz, V. Subotić, C. Hochenauer, R. Scharler, and A. Anca-Couce, "Solid oxide fuel cell operation with biomass gasification product gases: Performance- and carbon deposition risk evaluation via a CFD modelling approach," *Energy*, vol. 244, Apr. 2022, doi: 10.1016/j.energy.2021.123085.

[15] P. Qiu *et al.*, "A review on anode on-cell catalyst reforming layer for direct methane solid oxide fuel cells," *Int. J. Hydrogen Energy*, vol. 46, no. 49, pp. 25208–25224, 2021, doi: 10.1016/j.ijhydene.2021.05.040.

[16] D. Udomsilp *et al.*, "Metal-Supported Solid Oxide Fuel Cells with Exceptionally High Power Density for Range Extender Systems," *Cell Reports Phys. Sci.*, vol. 1, no. 6, 2020, doi: 10.1016/j.xcrp.2020.100072.

[17] C. A. Thieu *et al.*, "Effect of secondary metal catalysts on butane internal steam reforming operation of thin-film solid oxide fuel cells at 500–600 °C," *Appl. Catal. B Environ.*, vol. 263, no. July 2019, 2020, doi: 10.1016/j.apcatb.2019.118349.

[18] Q. Fu, Z. Li, Z. Liu, and W. Wei, "Performance Study of Solid Oxide Fuel Cell with Ni-Foam Indirect Internal Reformer: Intrinsic Reforming Kinetics and Temperature Uniformity," *SSRN Electron. J.*, vol. 457, no. December 2022, p. 141170, 2022, doi: 10.2139/ssrn.4211160.

[19] N. Jantakananuruk, J. R. Page, C. D. Armstrong, J. Persky, R. Datta, and A. R. Teixeira, "Integrated thermal reforming and electro-oxidation in

ammonia-fueled tubular solid oxide fuel cells toward autothermal operation," *J. Power Sources*, vol. 548, no. September, p. 231999, 2022, doi: 10.1016/j.jpowsour.2022.231999.

[20] J. Sang *et al.*, "Power generation from flat-tube solid oxide fuel cells by direct internal dry reforming of methanol: A route for simultaneous utilization of CO2 and biofuels," *Chem. Eng. J.*, vol. 457, no. December 2022, p. 141189, 2023, doi: 10.1016/j.cej.2022.141189.

[21] A. K. S. Iyengar, B. J. Koeppel, D. L. Keairns, M. C. Woods, G. A. Hackett, and T. R. Shultz, "Performance of a natural gas solid oxide fuel cell system with and without carbon capture," *J. Energy Resour. Technol. Trans. ASME*, vol. 143, no. 4, pp. 1–9, 2021, doi: 10.1115/1.4048247.

[22] E. Dogdibegovic, Y. Fukuyama, and M. C. Tucker, "Ethanol internal reforming in solid oxide fuel cells: A path toward high performance metal-supported cells for vehicular applications," *J. Power Sources*, vol. 449, no. June 2019, p. 227598, 2020, doi: 10.1016/j.jpowsour.2019.227598.

[23] S. A. Saadabadi, A. Thallam Thattai, L. Fan, R. E. F. Lindeboom, H. Spanjers, and P. V. Aravind, "Solid Oxide Fuel Cells fuelled with biogas: Potential and constraints," *Renew. Energy*, vol. 134, pp. 194–214, 2019, doi: 10.1016/j.renene.2018.11.028.

[24] M. LaBarbera, M. Fedkin, X. Wang, X. Chao, C. Song, and S. Lvov, "Solid Oxide Fuel Cell Fueled by Diesel Reformate and Anaerobic Digester Gas," *ECS Trans.*, vol. 35, no. 1, pp. 2867–2872, 2011, doi: 10.1149/1.3570286.

[25] X. Hou, O. Marin-Flores, B. W. Kwon, J. Kim, M. G. Norton, and S. Ha, "Gasoline-fueled solid oxide fuel cell with high power density," *J. Power Sources*, vol. 268, pp. 546–549, 2014, doi: 10.1016/j.jpowsour.2014.06.038.

[26] A. Singh and J. M. Hill, "Carbon tolerance, electrochemical performance and stability of solid oxide fuel cells with Ni/yttria stabilized zirconia anodes impregnated with Sn and operated with methane," *J. Power Sources*, vol. 214, pp. 185–194, 2012, doi: 10.1016/j.jpowsour.2012.04.062.

[27] J. B. Goodenough and Y. H. Huang, "Alternative anode materials for solid oxide fuel cells," *J. Power Sources*, vol. 173, no. 1, pp. 1–10, 2007, doi: 10.1016/j.jpowsour.2007.08.011.

[28] P. Qiu, X. Yang, S. Sun, L. Jia, J. Li, and F. Chen, "Enhanced electrochemical performance and durability for direct CH4–CO2 solid oxide fuel cells with an on-cell reforming layer," *Int. J. Hydrogen Energy*, vol. 46, no. 44, pp. 22974–22982, 2021, doi: 10.1016/j.ijhydene.2021.04.107.

[29] Z. Jiang, N. A. Arifin, P. Mardle, and R. Steinberger-Wilckens, "Electrochemical Performance and Carbon Resistance Comparison between Tin, Copper and Silver-Doped Nickel/Yttria-Stabilized Zirconia Anodes SOFCs Operated with Biogas," *J. Electrochem. Soc.*, vol. 166, no. 6, pp. F393–F398, 2019, doi: 10.1149/2.1011906jes.

[30] B. Illathukandy *et al.*, "Solid oxide fuel cells (SOFCs) fed with biogas containing hydrogen chloride traces: Impact on direct internal reforming and electrochemical performance," *Electrochim. Acta*, vol. 433, no. September, p. 141198, 2022, doi: 10.1016/j.electacta.2022.141198.

[31] N. A. Arifin, L. Troskialina, A. H. Shamsuddin, and R. Steinberger-Wilckens, "Effects of Sn doping on the manufacturing, performance and carbon deposition of Ni/ScSZ cells in solid oxide fuel cells," *Int. J. Hydrogen Energy*, vol. 45, no. 51, pp. 27575–27586, 2020, doi: 10.1016/j.ijhydene.2020.07.071.

[32] H. H. Faheem, S. Z. Abbas, A. N. Tabish, L. Fan, and F. Maqbool, "A review on mathematical modelling of Direct Internal Reforming- Solid Oxide Fuel Cells," *J. Power Sources*, vol. 520, no. November 2021, p. 230857, 2022, doi: 10.1016/j.jpowsour.2021.230857.

[33] L. Fan *et al.*, "Advances on methane reforming in solid oxide fuel cells," *Renew. Sustain. Energy Rev.*, vol. 166, no. March, p. 112646, 2022, doi: 10.1016/j.rser.2022.112646.

[34] W. J. Sembler and S. Kumar, "Optimization of a single-cell solid-oxide fuel cell using computational fluid dynamics," *J. Fuel Cell Sci. Technol.*, vol. 8, no. 2, pp. 1–12, 2011, doi: 10.1115/1.4002616.

[35] T. M. Gür, "Comprehensive review of methane conversion in solid oxide fuel cells: Prospects for efficient electricity generation from natural gas," *Prog. Energy Combust. Sci.*, vol. 54, pp. 1–64, 2016, doi: 10.1016/j.pecs.2015.10.004.

[36] Q. Xu *et al.*, "A comprehensive review of solid oxide fuel cells operating on various promising alternative fuels," *Energy Convers. Manag.*, vol. 253, p. 115175, Feb. 2022, doi: 10.1016/J.ENCONMAN.2021.115175.

[37] T. Wei, B. Liu, L. Jia, and R. Li, "Perovskite materials for highly efficient catalytic CH4 fuel reforming in solid oxide fuel cell," *Int. J. Hydrogen Energy*, vol. 46, no. 48, pp. 24441–24460, 2021, doi: 10.1016/j.ijhydene.2021.05.021.

[38] N. Wang, J. Y. H. Fuh, S. T. Dheen, and A. Senthil Kumar, "Synthesis methods of functionalized nanoparticles: a review," *Bio-Design Manuf.*, vol. 4, no. 2, pp. 379–404, 2021, doi: 10.1007/s42242-020-00106-3.

[39] M. Rafique, H. Nawaz, M. Shahid Rafique, M. Bilal Tahir, G. Nabi, and N. R. Khalid, "Material and method selection for efficient solid oxide fuel cell anode: Recent advancements and reviews," *Int. J. Energy Res.*, vol. 43, no. 7, pp. 2423–2446, 2019, doi: 10.1002/er.4210.

[40] N. H. Hadi, M. R. Somalu, A. A. Samat, A. Muchtar, N. A. Baharuddin, and M. Anwar, "A review on the preparation of anode materials and anode films for solid oxide fuel cell applications," *Int. J. Energy Res.*, vol. 45, no. 10, pp. 14357–14388, 2021, doi: 10.1002/er.6763.

[41] B. Shri Prakash, S. Senthil Kumar, and S. T. Aruna, "Properties and development of Ni/YSZ as an anode material in solid oxide fuel cell: A review," *Renew. Sustain. Energy Rev.*, vol. 36, pp. 149–179, 2014, doi: 10.1016/j.rser.2014.04.043.

[42] W. H. Kan, A. J. Samson, and V. Thangadurai, "Trends in electrode development for next generation solid oxide fuel cells," *J. Mater. Chem. A*, vol. 4, no. 46, pp.

17913–17932, 2016, doi: 10.1039/c6ta06757c.

[43] N. F. Raduwan, N. Shaari, S. K. Kamarudin, M. S. Masdar, and R. M. Yunus, "An overview of nanomaterials in fuel cells: Synthesis method and application," *Int. J. Hydrogen Energy*, vol. 47, no. 42, pp. 18468–18495, 2022, doi: 10.1016/j.ijhydene.2022.03.035.

[44] N. Baig, I. Kammakakam, W. Falath, and I. Kammakakam, "Nanomaterials: A review of synthesis methods, properties, recent progress, and challenges," *Mater. Adv.*, vol. 2, no. 6, pp. 1821–1871, 2021, doi: 10.1039/d0ma00807a.

[45] P. G. Jamkhande, N. W. Ghule, A. H. Bamer, and M. G. Kalaskar, "Metal nanoparticles synthesis: An overview on methods of preparation, advantages and disadvantages, and applications," *J. Drug Deliv. Sci. Technol.*, vol. 53, p. 101174, 2019, doi: 10.1016/j.jddst.2019.101174.

[46] J. Koettgen and M. Martin, "The ionic conductivity of Sm-doped ceria," *J. Am. Ceram. Soc.*, vol. 103, no. 6, pp. 3776–3787, 2020, doi: 10.1111/jace.17066.

[47] S. S. Itkulova, Y. A. Boleubayev, and K. A. Valishevskiy, "Multicomponent Co-based sol–gel catalysts for dry/steam reforming of methane," *J. Sol-Gel Sci. Technol.*, vol. 92, no. 2, pp. 331–341, 2019, doi: 10.1007/s10971-019-05110-3.

[48] A. M. Shaiful Bahari *et al.*, "Facile synthesis of Zr-based metal-organic gel (Zr-MOG) using 'green' sol-gel approach," *Surfaces and Interfaces*, vol. 27, no. December 2020, p. 101469, 2021, doi: 10.1016/j.surfin.2021.101469.

[49] J. Santos-Lorenzo *et al.*, "A straightforward route to obtain zirconium based metal-organic gels," *Microporous Mesoporous Mater.*, vol. 284, no. March, pp. 128–132, 2019, doi: 10.1016/j.micromeso.2019.04.008.

[50] B. Bueken *et al.*, "Gel-based morphological design of zirconium metal–organic frameworks," *Chem. Sci.*, vol. 8, no. 5, pp. 3939–3948, 2017, doi: 10.1039/C6SC05602D.

[51] Y. Ma, N. Fenineche, O. Elkedim, M. Moliere, H. Liao, and P. Briois, "Synthesis of apatite type La10−xSrxSi6O27−0.5x powders for IT-SOFC using sol–gel process," *Int. J. Hydrogen Energy*, vol. 41, no. 23, pp. 9993–10000, 2016, doi: 10.1016/j.ijhydene.2016.02.006.

[52] P. Xu;, Z. Zhou;, C. Zhao;, and Z. Cheng;, "Ni/CaO-Al2O3 Bifunctional Catalysts for Sorption-Enhanced Steam Methane Reforming," *AIChE J.*, vol. 60, no. 10, pp. 3547–3556, 2014, doi: DOI 10.1002/aic.14543.

[53] P. Xu, M. Xie, Z. Cheng, and Z. Zhou, "CO2 capture performance of CaO-based sorbents prepared by a sol-gel method," *Ind. Eng. Chem. Res.*, vol. 52, no. 34, pp. 12161–12169, 2013, doi: 10.1021/ie401600e.

[54] B. Bej, N. C. Pradhan, and S. Neogi, "Production of hydrogen by steam reforming of methane over alumina supported nano-NiO/SiO2 catalyst," *Catal. Today*, vol. 207, pp. 28–35, 2013, doi: 10.1016/j.cattod.2012.04.011.

[55] Z. Wang, G. M. Kale, and M. Ghadiri, "Sol-gel production of Ce 0.8 Gd 0.2 O 1.9 nanopowders using sucrose and pectin as organic precursors," *J. Am. Ceram. Soc.*, vol. 95, no. 9, pp. 2863–2868, 2012, doi: 10.1111/j.1551-2916.2012.05303.x.

[56] J. Zhao, X. Xu, W. Zhou, I. Blakey, S. Liu, and Z. Zhu, "Proton-conducting la-doped ceria-based internal reforming layer for direct methane solid oxide fuel cells," *ACS Appl. Mater. Interfaces*, vol. 9, no. 39, pp. 33758–33765, 2017, doi: 10.1021/acsami.7b07938.

[57] Y. Zhu, W. Fan, T. Zhou, and X. Li, "Removal of chelated heavy metals from aqueous solution: A review of current methods and mechanisms," *Sci. Total Environ.*, vol. 678, no. 37, pp. 253–266, 2019, doi: 10.1016/j.scitotenv.2019.04.416.

[58] L. Spiridigliozzi *et al.*, "Engineered co-precipitation chemistry with ammonium carbonate for scalable synthesis and sintering of improved Sm0.2Ce0.8O1.90 and Gd0.16Pr0.04Ce0.8O1.90 electrolytes for IT-SOFCs," *J. Ind. Eng. Chem.*, vol. 59, no. February, pp. 17–27, 2018, doi: 10.1016/j.jiec.2017.10.001.

[59] J. H. Kang, Y. M. Kim, H. S. Kim, M. S. Lee, J. H. Jang, and J. H. Jo, "Fabrication characteristics of SOFC single cell using nanocrystalline 1Ce10ScSZ electrolyte powder prepared by co-precipitation process," *J. Fuel Cell Sci. Technol.*, vol. 9, no. 1, pp. 1–6, 2012, doi: 10.1115/1.4003783.

[60] F. Kalyk *et al.*, "Comparative study of samarium-doped ceria nanopowders synthesized by various chemical synthesis routes," *Ceram. Int.*, vol. 46, no. 15, pp. 24385–24394, 2020, doi: 10.1016/j.ceramint.2020.06.221.

[61] K. Shetty, H. P. Nagaswarupa, D. Rangappa, K. S. Anantharaju, B. S. Surendra, and A. Kumar, "Comparison Study of Solgel and Combustion Method for Synthesis Nano Spinel MgFe2O4 and its Influence on Electrochemical Activity," *Mater. Today Proc.*, vol. 5, no. 10, pp. 22362–22367, 2018, doi: 10.1016/j.matpr.2018.06.603.

[62] Z. Ghahramani, A. M. Arabi, M. Shafiee Afarani, and M. Mahdavian, "Solution combustion synthesis of cerium oxide nanoparticles as corrosion inhibitor," *Int. J. Appl. Ceram. Technol.*, vol. 17, no. 3, pp. 1514–1521, 2020, doi: 10.1111/ijac.13365.

[63] W. Wang, R. Ran, and Z. Shao, "Combustion-synthesized Ru-Al2O3 composites as anode catalyst layer of a solid oxide fuel cell operating on methane," *Int. J. Hydrogen Energy*, vol. 36, no. 1, pp. 755–764, 2011, doi: 10.1016/j.ijhydene.2010.09.048.

[64] W. Wang *et al.*, "A NiFeCu alloy anode catalyst for direct-methane solid oxide fuel cells," *J. Power Sources*, vol. 258, pp. 134–141, 2014, doi: 10.1016/j.jpowsour.2014.02.008.

[65] H. Zhu, W. Wang, R. Ran, C. Su, H. Shi, and Z. Shao, "Iron incorporated Ni e ZrO 2 catalysts for electric power generation from methane," *Int. J. Hydrogen Energy*, vol. 37, no. 12, pp. 9801–9808, 2012, doi: 10.1016/j.ijhydene.2012.03.060.

[66] M. R. Somalu, W. N. A. Wan Yusof, A. Abdul Samat, N. W. Norman, A. Muchtar, and N. A. Baharuddin, "Synthesis and Characterization of Zn-doped LiCoO2 Material Prepared via Glycinenitrate Combustion Method for Proton Conducting Solid Oxide Fuel Cell Application," *J. Kejuruter.*, vol. SI1, no. 1, pp. 11–15, 2018, doi: 10.17576/jkukm-2018-si1(1)-02.

[67] H. Cheng, S. Chen, H. Liu, L. Jang, and S.-Y. Chang,

"Glycine–Nitrate Combustion Synthesis of Cu-Based Nanoparticles for NP9EO Degradation Applications," *Catalysts*, vol. 10, no. 9, p. 1061, Sep. 2020, doi: 10.3390/catal10091061.

[68] W. Wang *et al.*, "Effect of nickel content and preparation method on the performance of Ni-Al2O3 towards the applications in solid oxide fuel cells," *Int. J. Hydrogen Energy*, vol. 36, no. 17, pp. 10958–10967, 2011, doi: 10.1016/j.ijhydene.2011.05.109.

[69] P. Qiu *et al.*, "Redox-Reversible Electrode Material for Direct Hydrocarbon Solid Oxide Fuel Cells," *ACS Appl. Mater. Interfaces*, vol. 12, no. 12, pp. 13988–13995, 2020, doi: 10.1021/acsami.0c00922.

[70] J. Zhao, X. Xu, W. Zhou, and Z. Zhu, "An in situ formed MnO-Co composite catalyst layer over Ni-Ce0.8Sm0.2O2−x anodes for direct methane solid oxide fuel cells," *J. Mater. Chem. A*, vol. 5, no. 14, pp. 6494–6503, 2017, doi: 10.1039/c6ta10473h.

[71] C. Jin, C. Yang, F. Zhao, A. Coffin, and F. Chen, "Direct-methane solid oxide fuel cells with Cu1.3Mn 1.7O4 spinel internal reforming layer," *Electrochem. commun.*, vol. 12, no. 10, pp. 1450–1452, 2010, doi: 10.1016/j.elecom.2010.08.006.

[72] A. Samson Nesaraj and M. L. Reni, "Wet-Chemical Synthesis and Physico / Electro-Chemical Performance Characteristics of Novel Perovskite Cathode Materials for Low-Temperature Solid Oxide Fuel Cells," *Iran. J. Chem. Chem. Eng.*, vol. 40, no. 2, pp. 463–475, 2021, doi: 10.30492/ijcce.2019.37315.

[73] A. J. Majewski, S. K. Singh, N. K. Labhasetwar, and R. Steinberger-Wilckens, "Nickel–molybdenum catalysts for combined solid oxide fuel cell internal steam and dry reforming," *Chem. Eng. Sci.*, vol. 232, 2021, doi: 10.1016/j.ces.2020.116341.

[74] S. Dey *et al.*, "Facile synthesis of doped ceria-based oxide by co-precipitation technique and performance evaluation in solid oxide fuel cell," *Int. J. Appl. Ceram. Technol.*, vol. 17, no. 4, pp. 1769–1784, 2020, doi: 10.1111/ijac.13505.

[75] T. L. Gilbile, R. S. Pawar, V. N. Kapatkar, R. C. Kamble, and S. S. Pawar, "Synthesis and Performance Tuning of Sm 0.2 Ce 0.8 O 2−δ Electrolyte for Low Temperature Solid Oxide Fuel Cell Application," *J. Electron. Mater.*, vol. 48, no. 6, pp. 4117–4124, 2019, doi: 10.1007/s11664-019-07184-9.

[76] T. Li and Q. Shi, "Structure, morphology and electrical conductivity of Sm and Bi co-doped CeO2 electrolytes synthesized by co-precipitation method," *J. Mater. Sci. Mater. Electron.*, vol. 29, no. 16, pp. 13925–13930, 2018, doi: 10.1007/s10854-018-9525-y.

[77] C. E. Daza, S. Moreno, and R. Molina, "Co-precipitated Ni-Mg-Al catalysts containing Ce for CO2 reforming of methane," *Int. J. Hydrogen Energy*, vol. 36, no. 6, pp. 3886–3894, 2011, doi: 10.1016/j.ijhydene.2010.12.082.

[78] W. Wang, C. Su, Y. Wu, R. Ran, and Z. Shao, "A comprehensive evaluation of a Ni-Al2O3 catalyst as a functional layer of solid-oxide fuel cell anode," *J. Power Sources*, vol. 195, no. 2, pp. 402–411, 2010, doi: 10.1016/j.jpowsour.2009.07.053.